2

X-670-72-102

PREPRINT

NASA TM X 65873

THE ULTRAVIOLET FLUX ENVELOPES OF MAIN-SEQUENCE B STARS

ANNE B. UNDERHILL

(NASA-TM-X-65873) THE ULTRAVIOLET FLUX ENVELOPES OF MAIN-SEQUENCE B STARS A.B. Underhill (NASA) Apr. 1972 48 p CSCL 03B

N72-23889

Unclas

G3/30 25525

APRIL 1972

GSFC

GODDARD SPACE FLIGHT CENTER
GREENBELT, MARYLAND

THE ULTRAVIOLET FLUX ENVELOPES OF MAIN-SEQUENCE B STARS

Anne B. Underhill
NASA, Goddard Space Flight Center
Greenbelt, Maryland

Received: ______________________

Short Title: Ultraviolet Flux Envelopes of B Stars

THE ULTRAVIOLET FLUX ENVELOPES OF MAIN-SEQUENCE B STARS

Anne B. Underhill
NASA, Goddard Space Flight Center
Greenbelt, Maryland

ABSTRACT

Flux envelopes on an absolute energy scale from 1100 Å to 6000 Å prepared from OAO-II scans and from published ground-based material are presented for λ Leporis, B0.5 V η Ursae Majoris, B3 V, γ Ursae Majoris, A0 V, and α Lyrae, A0 V, and for α Canis Majoris A1 V from rocket scans. These, with already published flux envelopes for ζ Draconis, B6 III, and α Leonis, B7 V (Underhill 1972) are intercompared and compared with reference flux envelopes predicted by LTE theory from lightly line-blanketed model atmospheres. A considerable line blocking occurs at wavelengths shortward of 3000 Å with respect to the theoretical continuous spectra. The line blocking may be as much as 50 per cent at 1500 Å and between 1500 Å and 2500 Å it is comparable to that which exists in the sun between 3000 Å and 4000 Å.

Although γ Ursae Majoris, α Lyrae and α Canis Majoris have very similar visible spectra when viewed at low resolution, their ultraviolet spectra are significantly different, in particular α Lyrae shows an ultraviolet excess. Possible interpretations are discussed and attention is directed to

the fact that a spectral type assigned from ground-based colors or spectra is not necessarily a precise indicator of the details of the ultraviolet spectrum. Inclusion of line blocking of the magnitude found here into model atmosphere theories will modify theoretical relations between spectral type and effective temperature. It will also be significant for any precision theory of spectral line formation.

I. INTRODUCTION

The effective temperature of a star is by definition a measure of the total flux radiated by the star in all wavelengths per unit surface area. If the emergent flux from the star had the shape of a Planck function, the effective temperature would correspond to a real temperature, that of the equivalently radiating black body. However, the flux envelopes do not have the shapes of Planck functions thus the effective temperature can be regarded only as a measure of the integrated flux:

$$\sigma_R \; T_{eff}^4 = \pi \int_0^\infty F_\lambda \; d\lambda \tag{1}$$

where σ_R is Stefan's constant. The value of the flux integral is important for evaluating the luminosity of the star. If the stellar atmosphere may be represented locally by plane parallel layers, then

$$F_\lambda = 2 \int_{-\pi/2}^{+\pi/2} I_\lambda \; (0, \; \theta) \cos\theta \; \sin\theta \; d\theta, \tag{2}$$

where $I_\lambda \; (0, \; \theta)$ is the specific intensity emergent in a direction inclined at an angle θ to the local normal to the surface and the luminosity of the star is

$$L = 4\pi \; R^2 \sigma_R \; T_{eff}^4 \; . \tag{3}$$

If spherical geometry should be used to represent the atmosphere, the above relationship is not valid, cf. Cassinelli (1971).

One can observe only part of the flux envelope from a star. Various methods have been devised to deduce the effective temperature from the slope of the continuous spectrum over selected spectral ranges (colors), from the size of the Balmer jump and from the level of excitation and ionization shown by the spectrum in the range 3000 Å to 7000 Å. All of these methods have been calibrated in terms of effective temperature by means of synthesized spectra computed using the assumption of spectrum formation in LTE and model atmospheres stratified in plane parallel layers which are in hydrostatic equilibrium.

For B type model atmospheres one of the most consistent correlations is that between the computed Balmer jump and the effective temperature. There is also a consistent observed empirical relationship between spectral type and the Balmer jump (Chalonge and Divan 1952). By computing the theoretical equivalent of the observed Balmer jump one obtains a relationship between the empirically assigned spectral type and the effective temperature of the model. For B type main-sequence stars, this relationship is not dependent on log g. Since spectral type and $(B-V)_o$ are empirically related, one has also a relationship between $(B-V)_o$ and effective temperature.

If the theory used to synthesize spectra were unimpeachable, there should be no conflict between the values of effective temperature estimated from line spectra and from the Balmer jump or from colors. However, conflicting results are found, particularly for the Bp stars where the shape of the continuous spectrum frequently suggests a higher value of the effective temperature than does the line spectrum.

The purpose of this paper is to assemble flux envelopes from 1100 Å to 6000 Å for representative, nearby, thus unreddened, main-sequence stars and to compare these envelopes with the flux envelopes predicted from the classical LTE theory of model atmospheres in order to obtain insight concerning the meaning of the discrepancies between the effective temperatures deduced by various methods. Although Bless and Savage (1972) have indicated that unreddened stars of types B3 and earlier and in luminosity classes II-V have similar ultraviolet spectral distributions if their absorption-line spectral types are the same, it is not certain that these ultraviolet spectral distributions are the same as the ultraviolet flux envelopes predicted by model atmospheres which give a flux envelope which fits in the 4000 Å to 6000 Å region. This point is investigated here for stars of types B0.5 V to A1V and it is found that the observed ultraviolet flux envelopes fall significantly below the envelopes predicted from lightly line-blanketed models.

Broad-band photometry has been used by Davis and Webb (1970) to demonstrate the ultraviolet flux discrepancy of stars of types B8 to F5 relative to the predicted fluxes from lightly line-blanketed model atmospheres. Campbell (1971) has also compared broad-band filter photometry of stars in the ultraviolet with theoretical predictions. A significant ultraviolet flux discrepancy, probably due to line blanketing, is found by Davis and Webb while Campbell concludes that there is good agreement with the predictions of lightly line-blanketed models, at least for types earlier than B5. However, there is a large scatter in Campbell's results. It is uncertain how much of the scatter is due to intrinsic differences between the stars themselves, how much is due to variations in the interstellar extinction and how much is due to observational error or misclassification.

It is of importance to define more accurately the discrepancies, if any, between the ultraviolet flux envelopes of stars and theoretical predictions. Significant ultraviolet line blanketing for B stars implies increased back warming in the stellar atmosphere with effects on the normally observed spectrum that have not been considered heretofore. In addition, the energy balance in interstellar space may be modified from that deduced to result from irradiation by stars which radiate like the available model atmospheres.

Finally the ultraviolet fluxes of γ Ursae Majoris, α Lyrae and α Canis Majoris are compared and shown to differ significantly although their continuous spectra observed by means of ground-based instruments are very similar one to the other.

II. STARS OBSERVED AND OBSERVATIONAL MATERIAL USED

The stars observed and the sources for the ground-based scans are given in Table 1. The color excesses are with reference to the intrinsic B-V colors of Johnson (1963). None of these stars appears to be reddened significantly by interstellar dust and in what follows possible modification of the stellar flux distribution by interstellar dust will be ignored. The ground-based spectrum scans are published as relative energy distributions. They have been converted to absolute energy, $\mathcal{F}_\lambda$, in units of erg cm^{-2} s^{-1} Å^{-1} received at the earth using the V magnitude and the equivalent of V = 0.00 in energy units given by Oke and Schild (1970). The relative flux distribution for α Lyrae of Hayes (1970) has been transformed to the Oke and Schild (1970) system. The observations of Hardorp and Scholz (1970) are left unmodified. They use the same instrument as Oke and Schild and record at the same wavelengths.

The ultraviolet flux envelope of all the stars except α Canis Majoris has been obtained with the spectrum scanners of the Wisconsin Experiment Package on OAO-II. The spectrum scanners and their use are described by Code et al. (1970) and by Bless and Savage (1972). The nominal spectral resolution of Scanner 1 is 20 Å and data are obtained at steps separated by about 20 Å over the range 3700 Å to 1815 Å. The spectrum from 1100 Å to nearly 1800 Å in steps of about 10.5 Å is covered by Scanner 2 at approximately 10 Å resolution. The wavelength of each grating step of Scanner 1 was determined using a relation provided by B.D. Savage. The zero-point is set by determining which grating step corresponds to the center of the absorption dip due to the Mg II resonance lines. This point is assigned the wavelength 2800 Å. In the cases where the Mg II dip is not well determined, grating step 50 was set to 2800 Å. In these cases (λ Leporis and η Ursae Majoris) the wavelengths may be in error by ± 20 Å or possibly ± 40 Å. Wavelengths in the range of Scanner 2 were determined using the interpolation formula derived by Underhill, Leckrone and West (1972). In each case the observations were made when the boresight tracker was holding the spacecraft pointed at the target. This ensures that the wavelength-grating step relationship is the same as that derived by Underhill, Leckrone and West. Some of the present scans are those used in the earlier paper. The error in wavelength of any observed point using Scanner 2 should be at most about 7 Å.

The data obtained with Scanner 1 were converted to relative intensities using the sensitivity curve derived for Scanner 1 by Underhill (1972). This curve is a modification of a preliminary sensitivity curve provided by B.D. Savage. The modification is such as to make the absolute intensities of α Leonis in the range 1800 Å to 3700 Å coincide with the absolute energies derived by Evans (1971) from rocket-borne spectrometer scans. The relative energies derived from Scanner 1 are put on an absolute scale by making the Scanner 1 results coincide in their region of overlap with the absolute energies obtained from the ground-based scans. The data obtained with Scanner 2 were converted to absolute energies using a sensitivity curve derived by Leckrone (private communication) by comparing recent OAO-II Scanner 2 observations of κ Orionis, B0Ia, and α Leonis, B7V, with the absolute energy distributions of Evans (1971). The absolute energies at wavelengths shorter than about 1800 Å are thus on a scale which is independent of the absolute calibration of the ground-based scans.

The date of each OAO-II observation is listed in Table 2. In each case only observations made when the spacecraft is in night and free from the South Atlantic Anomaly are used. (Bless and Savage (1972) discuss the precautions which are necessary in order to select good data.) An appropriate background count has been subtracted from the gross count in each case. The results are presented in Section IV. In each spectral range they represent the average of all available data for each star. The star α Canis Majoris is too bright for OAO-II. The spectral scan obtained with a rocket-borne spectrometer by Stecher (1970) and the results of Evans (1971) are used to represent the ultraviolet flux of this star.

III. THE THEORETICAL FLUX DISTRIBUTIONS USED

The chief grid of predicted fluxes with which the observed flux envelopes have been compared is that of Klinglesmith (1971) for a composition X = 2/3, Y = 1/3 and log g = 4.0 This material has been supplemented by unpublished models computed with the same program but at different effective temperatures. The opacity sources in these LTE model atmospheres are electron scattering, bound-free absorption from H, H^-, He I, He II and He^- and lines of the Lyman and Balmer series of hydrogen. In addition a few unpublished models, effective temperatures between 9500°K and 10000°K, in which absorption due to Si I is added are used. The flux envelopes from LTE model atmospheres of Van Citters and Morton (1970) with composition N(He)/N(H) = 0.15 and log g = 4.0 in which the opacity is due to electron scattering, bound-free absorption from H, H^-, He I and He II as well as from 98 lines of H and heavier ions at wavelengths shortward of 2300 Å have also been used. It turns out that the continuous flux distribution in regions free from lines is very nearly the same in both sets of models when models with the same composition, T_{eff} and log g are compared. This is because at the levels from which the continuous spectrum comes both sets of models, for the same parameters, have about the same temperature-pressure structure. Both sets of models can be characterized as lightly line-blanketed.

The predicted F_λ from the models must be normalized to the observed stellar fluxes at the earth to allow for the size of the star and for the dilution of radiation resulting from the distance of the star. This is done by fitting logarithmic plots of the predicted fluxes to logarithmic plots of the observed fluxes over the range 4000 Å to 6000 Å. This spectral range is chosen because here there are very few lines to distort the observed fluxes from the shape of fluxes predicted with all lines but the hydrogen lines ignored. The fitting factor is

$$\frac{\pi F_\lambda}{\mathcal{F}_\lambda} = \frac{d^2}{R^2} , \tag{4}$$

where d is the distance to the star and R is the stellar radius. With the fitting factor determined in this way the model flux is scaled to the observed flux. A representative model, discussed below, has been selected for each star. The scaled theoretical flux distribution is shown in each figure as a continuous line.

The scaling factors for the models result in radii which are consistent with existing measures or estimates of the radii of main-sequence stars of types B0.5 to A1. This consistency check is summarized in Table 3 where the estimated distance and the resulting radius for each star is given. The distances of α Lyrae and α Canis Majoris are estimated from parallaxes; the distances of the other stars are estimated from the M_V corresponding to their spectral type (Blaauw 1963). Radii from the interferometer measurements of Hanbury Brown et al. (1967) are given in the last column. The quoted standard deviation corresponds to the uncertainty in the parallax. The results for ζ Draconis and α Leonis have been discussed by Underhill (1972) where it is shown that the above method of estimating stellar radii is a valid method so long as there is no interstellar extinction.

IV. COMPARISON OF OBSERVED AND PREDICTED FLUXES

a) λ Leporis, B0.5 V

In Figures 1 and 2 the observed flux envelope of λ Leporis is compared with the predicted flux envelope from a Van Citters and Morton (1970) model with the parameters N(He)/N(H) = 0.15, θ_e = 0.200 and log g = 4.0. The selected model fits the observed flux envelope reasonably well between 4000 Å and 6000 Å. In the near ultraviolet (2700 Å to 3600 Å) the star is brighter than the model. At wavelengths shorter than 2200 Å a large flux discrepancy occurs. The apparent excess brightness of λ Leporis in the near ultraviolet may be fictitious owing to a possible error in fitting within the short overlap with the ground-based observations and to using too cool a model. The scaling to absolute energies of the ground-based and Scanner 1 data seems to be reasonable, for the radius of λ Leporis (Table 3) is in the expected range.

The Scanner 2 data are on an independently determined absolute energy scale. Even if there was a 25 per cent error in the absolute calibration of Scanner 2 in the direction of the observed fluxes being too small, the observed fluxes would fall significantly below the predicted fluxes. Such a large error in the adopted energy calibration is not expected (Evans 1971). Thus at wavelengths shortward from 2200 Å there is a real, large discrepancy in comparison to the predictions from a lightly line-blanketed model atmosphere.

No correction has been made to allow for interstellar reddening because E(B-V) is zero. Hardorp and Scholz (1970) have discussed the possible reddening of λ Leporis and they conclude that it is small. At a distance of 455 pc (Table 3) a small amount of reddening might be present. Interstellar extinction would reduce the flux deficit found in the ultraviolet by a small and, at present, undeterminable amount. On the other hand, according to the detailed spectrum analysis of

Hardorp and Scholz, the atmosphere of λ Leporis may be represented satisfactorily by an unblanketed model atmosphere with $T_{eff} = 30900^{o}K$ and log g = 4.05. Since a predicted flux envelope for such a model was not available, comparison has been made with the flux envelope for a model with T_{eff} = $25200^{o}K$. Increasing the effective temperature of the model would increase the ultraviolet flux discrepancy because the model would become brighter in the ultraviolet relative to its brightness in the visible range. An increase in effective temperature would decrease the excess brightness found in the near ultraviolet and would reduce the radius of the star.

The Scanner 2 data have sufficient spectral resolution to show absorption "lines". Each "line" is in reality a blend of several lines; the major contributors can be identified from Table 1 of Underhill, Leckrone, and West (1972). The ratio of the stellar flux envelope to that of the selected model is shown in Figure 3. The curves in Figure 3 were obtained by reading the observed flux envelopes and the predicted envelopes every 200 Å between 1300 Å and 5500 Å and taking ratios.

b) <u>η Ursae Majoris, B3 V</u>

The observed flux envelope of η Ursae Majoris is shown in Figure 4. The peak of the predicted flux envelope is shown in the inset at a reduced scale. The flux envelope from the selected model, which is a Klinglesmith (1971) model with parameters (18000^{o} , 4.0, 2/3, 1/3), fits the ground-based observations well, but an ultraviolet flux discrepancy begins at about 2800 Å. Kodaira (1970) has shown that the predicted visible spectrum from an unblanketed model with T_{eff} = 18000^{o}K, log g = 4.5 fits the ground-based observations of the continuous spectrum of η Ursae Majoris. The fitting of the OAO-II Scanner 1 results to the ground-based results is uncertain because the slopes of the two distributions differ widely in the region of overlap. The flux of the star relative to that of the reference model is shown in Figure 3. There is a large ultraviolet flux deficiency. No correction for interstellar reddening is warranted.

The Scanner 2 data reveal a number of absorption "lines" the major contributors to which can be found in Underhill, Leckrone, and West (1972). The relative intensity of the various lines is different than for λ Leporis; in particular the prominence of the resonance multiplet of Sc III at 1605 Å is striking.

Absolute ultraviolet fluxes for η Ursae Majoris have been measured by Opal et al. (1968) using a rocket-borne spectrometer. The monochromatic fluxes derived from Figure 2 of Opal et al. (read at 100 Å intervals) are given in Table 4 together with values read from Figure 4 with the scaled predicted fluxes from the reference model atmosphere. The measurements are in reasonable accord considering the uncertainties in both absolute calibrations. The observed ultraviolet fluxes are significantly lower than the predicted flux. Reference to the temperature scale for B type stars derived by Morton and Adams (1968) and to that derived by Heintze (1969) shows that a lightly line-blanketed model atmosphere with an effective temperature of 18000° should be representative for B3 main-sequence stars.

c) ζ Draconis, B6 III, and α Leonis, B7 V

The flux envelopes of ζ Draconis and α Leonis have been presented in Underhill (1972) where the selection of representative models is discussed fully. The observed flux envelopes have been compared with Klinglesmith models with the parameters (14000°, 4.0, 2/3, 1/3) and (13000°, 4.0, 2/3, 1/3) respectively. Significant ultraviolet flux discrepancies occur as is shown in Figure 3.

d) γ Ursae Majoris, A0 V

The observed flux envelope of γ Ursae Majoris is shown in Figure 5 together with the predicted flux envelope from an unpublished Klinglesmith model with the parameters $T_{eff} = 9750°$, log g = 4.0, X = 0.70034, Y = 0.27812, and $X_{Si} = 0.02154$. This model fits the ground-based observations of Schild, Peterson and Oke (1971) quite well in the region 4000 Å to 6000 Å . The resulting scaling factor together with the adopted visual absolute magnitude leads to an acceptable value for the radius of the star, see Table 3. The predicted flux in the spectral range 3700 Å to 3300 Å is about 10 per cent brighter than the observed flux. There is no obvious explanation for this discrepancy but Dr. Klinglesmith thinks some of his opacity routines may not be sufficiently accurate when the temperature is near 10000°. A higher temperatures his results agree well with those of others. The Klinglesmith models are computed using LTE theory. In spectral regions where the adopted opacity is large, for instance at the beginning of the Balmer continuum, more elegant computing routines might be required to obtain precise agreement with observations. In spite of the small discrepancy at the Balmer jump, the adopted reference model appears to represent well the Paschen continuum of an A0 V star between 4000 Å and 6000 Å. We shall assume that the predicted ultraviolet flux is representative for a star having the sources of opacity included in the adopted model.

Deep in the wing of Lyman α the observed flux and the predicted flux agree well. However, this agreement may be fortuitous owing to the statistical uncertainty of the results shortward of 1400 Å. At wavelengths longward of 1500 Å there is a significant flux discrepancy with respect to the reference flux envelope. Unfortunately no observations are available for this A0 V star in the near ultraviolet range covered by Scanner 1. The relative flux distribution of γUrsae Majoris with respect to the reference distribution is shown in Figure 3.

e) α Lyrae, A0 V

The flux envelope for α Lyrae derived from OAO-II and ground-based observations is shown in Figure 6. The reference flux envelope given by a continuous line, is the same as for γ Ursae Majoris but scaled to fit α Lyrae. It fits the ground-based observations quite well except for the discrepancy at the Balmer jump discussed above. The predicted flux for α Lyrae given by Schild, Peterson and Oke (1971) is shown by a broken line. It fits the ground-based observations even better. That model has $T_{eff} = 9650^{o}$, log g = 4.05 and the sources of opacity are those used in the Atlas program of Kurucz (1970) including continuous opacity from C I and N I. The overlap of the OAO-II Scanner data with the two sets of ground-based data is not too good but it probably leads to an uncertainty of less than 10 per cent in the absolute energies of the Scanner 1 results. The Scanner 2 results are based on the independent absolute energy calibration that is used for the other stars.

There is an important difference between the ultraviolet fluxes of the A0 V stars γ Ursae Majoris and α Lyrae. At wavelengths shortward of 1650 Å α Lyrae is brighter than the reference flux distribution from the Klinglesmith model while γ Ursae Majoris is fainter. This difference and the differences between the two computed flux distributions are discussed in Section VI. The relative flux distribution of α Lyrae with respect to the Klinglesmith distribution is shown in Figure 7. Most of the prominent "lines" which appear in the far ultraviolet spectra of γ Ursae Majoris and α Lyrae are due to the singly ionized elements.

The radius shown in Table 3, column 5 is from the fit to the Klinglesmith model. The fit to the Schild, Peterson and Oke model gives 2.83 solar radii.

f) α Canis Majoris, Al V

An ultraviolet flux envelope of α Canis Majoris has been published by Stecher (1970) and one has been given by Evans (1971). These envelopes are generally the same when allowance is made for the fact that although both scans are obtained with 10 Å resolution, but different absolute calibrations, Stecher presents his data read at frequent intervals whereas Evans averages over intervals of 100 Å and presents only the averaged results for a 100 Å wide band. The flux envelope for α Canis Majoris is shown in Figure 8. Stecher's published curves were read each 100 Å and the particular flux at the selected wavelength is plotted. The ground-based observations are due to Schild, Peterson and Oke (1971). The reference flux distribution is from the Klinglesmith model with $T_{eff} = 9750^{o}$ used for γ Ursae Majoris. When this model is scaled to the ground-based observations the resulting radius (Table 3) is almost identical with that measured by Hanbury Brown et al. (1967). The fit in the Paschen continuum is not so good as for the A0 V stars. Schild, Peterson and Oke (1971) suggest using a model with $T_{eff} = 10200^{o}$, log g = 4.35 but they published no flux distribution. Heintze (1968) also suggests an effective temperature over 10000^{o} whereas Strom, Gengerich and Strom (1966) have suggested an effective temperature near 9500^{o}. We conclude that the selected reference model is representative for α Canis Majoris with the proviso that the ultraviolet flux at wavelengths shortward of 2400 Å may be underestimated.

A fully line-blanketed model atmosphere having $T_{eff} = 10000^{o}$, log g = 4.0 has been considered by Maran, Kurucz , Strom and Strom (1968) to be representative of early A stars. Thanks to Dr. Maran access was obtained to the computer output of the emergent spectrum in the region 2000 Å to 3000 Å. The continuous spectrum given there was scaled to the star α Canis Majoris by means of the known distance and radius. The results are shown in Figure 8 by a broken line. This continuous spectrum lies considerably below that of the Klinglesmith model. Unfortunately a longer stretch of predicted spectrum from the Maran-Kurucz -Strom-Strom model is not available. Clearly, however, the flux from this model gives little indication of joining up with the ground-based observations at 3300 Å. Since the distance to Sirius is well known and the radius of Sirius is well known, the scaling factor is not uncertain. The MKSS model cannot be considered to be representative for Sirius even though it is an attractive model from the viewpoint that an explicit attempt has been made to take account of the full line blocking that may occur.

The flux distribution for Sirius relative to the selected reference spectrum shows a distinct ultraviolet brightening in comparison to the A0 V star γ Ursae Majoris, see Figure 7. However, at no wavelength is Sirius significantly brighter than the reference flux distribution. If a slightly hotter, lightly line-blanketed model were used, the predicted flux shortward of 1800 Å would be increased leading to an even greater flux deficit than is shown in Figure 7.

V. DISCUSSION

The relative stellar flux envelopes shown in Figures 3 and 7 summarize the results of this investigation. In general the predicted fluxes from the lightly blanketed models represent well the observed spectral distributions from 3300 Å to 6000 Å. A depression due to the overlap of the Balmer lines shortward of 3800 Å is visible. The predicted fluxes are calculated in detail for this region but they would have to be averaged over the scanner pass band of 50 Å to permit a detailed comparison with observations in the range 3647 Å to 4000 Å. The reality of the apparent flux excess at 2900 Å in the case of λ Leporis has already been commented upon.

The most characteristic trait of the observed flux curves relative to predicted flux curves from representative lightly blanketed model atmospheres is the increasing line blocking as one goes to shorter wavelengths. Only in the A stars does this trend reverse shortward of 2000 Å. At 1500 Å the precentage of the predicted light available is 61, 50, 49, 53, 69 and 87 for λ Leporis, η Ursae Majoris, ζ Draconis, α Leonis, γ Ursae Majoris and α Canis Majoris respectively. In the case of α Lyrae, at 1500 Å the star is 53 per cent <u>brighter</u> than the selected reference model predicts. A careful check has been made of the orientation of the entrance slot on the sky during the OAO-II Scanner 2 observations of α Lyrae and no B stars of detectable brightness were found to lie in the field of view. The excess brightness in the far ultraviolet of α Lyrae is real and it must be attributed to α Lyrae.

The severe ultraviolet line blanketing of B type stars demonstrated by these observations is to be expected when one considers the vast number of intrinsically strong lines which occur in ultraviolet B type spectra (see Smith 1969 and the references given there; also Smith 1970 and 1972).

In the solar spectrum in the range 3000 Å to 4000 Å where the line density is very great, the line blocking averages 40 to 50 per cent of the "continuous" light (Houtgast and Namba 1968). A line blocking of the magnitude found here in the ultraviolet spectrum of B and early A stars is comparable to that which exists for G stars in the ground-based ultraviolet spectrum.

A comparison of the far UV flux from ϵ Persei, B0.5 V, with the predicted flux from the Van Citters and Morton model used here has been made by Lillie et al. (1972). This group deduces a much smaller amount of line blanketing than is found here. The reason for their result (Lillie, private communication) is that they have applied to the predicted flux a correction for interstellar extinction corresponding to the average ultraviolet extinction curve of Bless and Savage (1972) for an E(B-V) of 0.1 mag. Otherwise their procedure is equivalent to what has been done here. The star ϵ Persei is an unsuitable candidate for making a comparison between theory and observation because the amount of interstellar extinction is critical and it cannot be determined precisely enough from the available information. The sky in the direction of ϵ Persei is mottled with interstellar clouds (Heechen 1951, Lynds 1969) and even though ϵ Persei seems to be no more than 200 to 300 pc distant, one cannot be sure what the extinction in front of ϵ Persei is.

The E(B-V) with reference to the normal color for type B0.5 V is not a reliable guide to the extinction because ϵ Persei is a double-lined spectroscopic binary (Petrie 1958) and the spectral type of the companion is not known. That the type is later than B0.5 is indicated by the fact that the E(U-B) with respect to the color of a B0.5 V star is only 0.03 although (E(B-V) is 0.10. Normally E(U-B) = 0.72 E(B-V). The spectral distribution given by Schild, Peterson and Oke (1971) for ϵ Persei fits the selected reference flux distribution well from 3300 Å to 4400 Å but it becomes appreciably brighter than the reference flux distribution at longer wavelengths. The observed UBV colors, the scanner results and spectrographic observations available at present do not permit one to determine accurately how much of the reddening is due to light from a companion of spectral type later than B0.5 V and how much is due to interstellar extinction. In view of this indeterminacy and the conclusion of Hardorp and Scholz (1970) that type B0.5 V (λ Leporis) corresponds to an effective temperature higher than 25200°, the conclusions of Lillie _et al._ concerning the amount of line blanketing at type B0.5 V must be regarded with reserve.

The observed differences between the ultraviolet spectra of γ Ursae Majoris, A0 V, α Lyrae, A0 V, and α Canis Majoris, A1 V, raise questions which cannot be answered with the present observational material. The star γ Ursae Majoris rotates rapidly with $\underline{v} \sin \underline{i}$ = 167 ± 7 kms^{-1} (Bernacca and Perinotto 1971) whereas α Lyrae and α Canis Majoris have $\underline{v} \sin \underline{i}$ equal to 5 ± 5 km s^{-1} and 10 ± 5 km s^{-1} respectively (Bernacca and Perinotto 1970). The precise value of the emergent flux at wavelengths shortward of 2000 Å for models with effective temperature near 9700°K is quite sensitive to the adopted opacity sources in that wavelength region and to the computing routines used, as the differences between the two predicted flux distributions displayed in Figure 6 shows. Whether it is also very sensitive to the projected rotational velocity is unknown at this time.

If the total radiative energy of γ Ursae Majoris, α Lyrae and α Canis Majoris can be represented by an effective temperature of 9750°K, then integration under the observed flux envelopes shows that 23 per cent of the stellar energy is emitted between 1100 Å and 3600 Å in the case of γ Ursae Majoris and 29 per cent in the case of Vega and of Sirius. The difference in <u>shape</u> between the ultraviolet flux envelopes of these three stars has already been commented upon. There are some reasons for suspecting that Vega may be a spectroscopic binary (<u>cf</u>. Petrie 1964). It is possible that the difference between the ultraviolet spectrum of γ Ursae Majoris and of α Lyrae is due to Vega being composed of an A0 V and a B9 V star, but the data are inadequate for proving this is so. The white dwarf companion of Sirius would not contribute enough energy to be observable in the ultraviolet owing to its small size (Greenstein, Oke and Shipman 1971). Thus, the reason for the difference between Sirius and γ Ursae Majoris is not yet clear.

VI. SUMMARY

Flux envelopes of unreddened main-sequence stars of spectral types B0, B3, A0 and A1 from 1100 Å to 6000 Å have been constructed using observations made with the spectrum scanners of the Wisconsin Experimental Package on OAO-II and published scans made with ground-based equipment. The ultraviolet observations have been put on an absolute scale by comparing with absolute energy spectrum scans of two stars obtained (Evans 1971) from rocket-borne spectrometers. The ground-based observations are on the absolute energy scale of Oke and Schild (1970). These observed flux envelopes and those published (Underhill 1972) for ζ Draconis, B6 III, and α Leonis, B7 V, have been compared with the flux envelopes predicted by means of lightly line-blanketed model atmospheres. A line blocking of up to 50 per cent is found at 1500 Å relative to the predictions from lightly blanketed models. This blocking is comparable to the line blocking in the solar spectrum between 3000 Å and 4000 Å (Houtgast and Namba

1968). Comparison with existing independently calibrated ultraviolet spectral scans suggests that the present observations are not seriously in error at wavelengths greater than 1500 Å. The problem of establishing standards of absolute energy in the rocket and satellite ultraviolet is still acute and more work needs to be done in this field, particularly at wavelengths shortward of 2000 Å.

More work needs to be done also on obtaining more truly representative model atmospheres for B stars. The strong line blocking demonstrated to be present will affect the structure of model atmospheres for it introduces additional sources of opacity which have not been adequately included in any sets of models presently available. In many cases the process of line formation will be modified by this line blocking from the simple concepts of the LTE theory which is used because the balance of radiative depopulation or population of the levels from which the observed lines occur can be modified by the shape of the actual radiation field in the range 1000 Å to 3000 Å in the relatively low density parts of the atmosphere where the lines are formed (Underhill 1970). Only in those cases where the level populations are strictly collision controlled will the effects of line blanketing on the observed level populations and ionization balance be negligible. It is not only the line transitions between various levels which are important, but also the radiative ionization from excited levels. The latter process can proceed at a significantly different rate in an atmosphere where the relevant radiation field has been depleted by a factor two or more over that commensurate with LTE. The present observations indicate that renewed attention to these problems is required if the part of the spectrum visible from the ground is to be used as an accurate index of what the ultraviolet spectrum may be expected to be. That the visible spectrum is insensitive to factors which are significant to the ultraviolet spectrum is clearly shown by the present comparison of the observations for γ Ursae Majoris, α Lyrae, and α Canis Majoris. It is perhaps not inappropriate to wonder how many of the "local" variations in the shape of the interstellar reddening law found by Bless and Savage (1972) from OAO-II observations are due to similar causes as those affecting γ Ursae Majoris, Vega and Sirius.

The actual shape of the ultraviolet spectrum of B and A stars may well be an important factor in determining the strength of the spectrum peculiarities which lead to Bp and Ap spectral types. It surely is relevant when one considers the contribution to the energy balance of the interstellar medium by radiation from B stars and the appearance of the ultraviolet spectrum of a galaxy viewed from the outside.

My sincere thanks go to Dr. A.D. Code of the University of Wisconsin for permission to use observations obtained with the Wisconsin Experimental Package on OAO-II, to Dr. D.S. Leckrone of the Goddard Space Flight Center for assembling most of the data for me and for providing the wavelength and intensity calibrations for the Scanner 2 material. The Scanner 1 material was made available to me on a Guest Observer Project approved while I was at the University of Utrecht. I am grateful to Dr. B.D. Savage of the University of Wisconsin for a preliminary relative sensitivity curve of Scanner 1 and for a wavelength calibration formula. My studies have been made easier by access to the absolute calibration work of D.C. Evans at the Goddard Space Flight Center and to the abundant model atmosphere and predicted spectrum output provided freely by Dr. D.A. Klinglesmith.

REFERENCES

Bernacca, P.L. and Perinotto, M. 1970, Contrib. Oss. Astrofys. Padova in Asiago, No. 239.

Bernacca, P.L. and Perinotto, M. 1971, Contrib. Oss. Astrofys. Padova in Asiago, No. 249; see table on Be and shell stars.

Blaauw, A. 1963, in Basic Astronomical Data, ed. K. Aa. Strand (Chicago: University of Chicago Press), p. 383.

Bless, R.C. and Savage, B.D. 1972, Ap.J., 171, 293.

Campbell, J.W. 1971, Ap.J., 165, 265.

Cassinelli, J.P. 1971, Ap.J., 165, 265.

Chalonge, D. and Divan, L. 1952, Ann. Ap., 15, 201.

Code, A.D., Houck, T.E., McNall, J.F., Bless, R.C. and Lillie, C.F. 1970, Ap.J., 161, 377.

Davis, J. and Webb, R.J. 1970, Ap.J., 159, 551.

Evans, D.C. 1971, Proc. OAO-II Symposium at Amherst, Mass., NASA-SP in press.

Greenstein, J.L., Oke, J.B. and Shipman, H.L. 1971, Ap.J., 169, 563.

Hanbury Brown, R., Davis, J., Allen, L.R. and Rome, J.M. 1967, M.N., 137, 393.

Hardorp, J. and Scholz, M. 1970, Ap.J. Suppl., 19, 193.

Hayes, D.S. 1970, Ap.J., 159, 165.

Heeschen, D.S. 1951, Ap.J., 114, 132.

Heintze, J.R.W. 1968, B.A.N., 20, 1.

Heintze, J.R.W. 1969, B.A.N., 20, 154.

Houtgast, J. and Namba, O. 1968, B.A.N., 20, 87.

Johnson, H.L. 1963, in Basic Astronomical Data, ed. K. Aa. Strand (Chicago: University of Chicago Press), p. 204.

Kodaira, K. 1970, Ap.J., 159, 931.

Kurucz, R.L. 1970, Atlas: A Computer Program for Calculating Model Stellar Atmospheres (Smithsonian Astrophysical Observatory Special Report 309).

Klinglesmith, D.A. 1971, Hydrogen Line Blanketed Model Stellar Atmospheres, NASA SP-3065.

Lillie, C.F., Bohlin, R.C., Molnar, M.R., Barth, C.A. and Lane, A.L. 1972, Science, 175, 321.

Lynds, B.T. 1969, Pub. Astron. Soc. Pacific, 81, 496.

Maran, S.P., Kurucz, R.L., Strom, K.M. and Strom, S.E. 1968, Ap.J., 153, 147.

Morton, D.C. and Adams, T.F. 1968, Ap.J., 151, 611.

Oke, J.B. and Schild, R. 1970, Ap.J., 161, 1015.

Opal, C.M., Moos, H.W., Fastie, W.G. and Bottema, M. 1968, Ap.J. (Letters), 153, L179.

Petrie, R.M. 1958, M.N., 118, 80; see specially p. 83.

Petrie, R.M. 1964, Pub. Dominion Astrophys. Obs., 12, 317, see particularly p. 331.

Schild, R., Peterson, D.M. and Oke, J.B. 1971, Ap.J., 166, 95.

Smith, A.M. 1969, Ap.J., 156, 93.

Smith, A.M. 1970, Ap.J., 160, 595.

Smith, A.M. 1972, Ap.J., 172, 129.

Stecher, T.P. 1970, Ap.J., 159, 545.

Strom, S.E., Gingerich, O. and Strom, K.M. 1966, Ap.J., 146, 880.

Underhill, A.B. 1970, in Spectrum Formation in Stars with Steady-State Extended Atmospheres, (NBS Special Publication 332), p. 3.

Underhill, A.B. 1972, Ap.J. in press

Underhill, A.B., Leckrone, D.A. and West, D.K. 1972, Ap.J., 171, 63.

Van Citters, G.W. and Morton, D.C. 1970, Ap.J., 161, 695.

TABLE 1

The Stars Observed with OAO-II

HR No.	Name	Spectral Type	V	B-V	E(B-V)	Source Ground-Based Scan
1756	λ Lep	B0.5 V	4.28	-0.28	0.00	1
5191	η UMa	B3 V	1.86	-0.20	0.00	2
6396	ζ Dra	B6 III	3.20	-0.15	-0.01	2
3982	α Leo	B7 V	1.36	-0.11	+0.01	2
4554	γ UMa	A0 V	2.44	+0.00	+0.00	2
7001	α Lyr	A0 V	0.04	+0.00	+0.00	3, 4
2491	α CMa	A1 V	-1.47	+0.01	-0.02	2

(1) Hardorp and Scholz (1970); (2) Schild, Peterson and Oke (1971); (3) Hayes (1970); (4) Oke and Schild (1970).

TABLE 2

The Dates (U.T.) of the OAO-II Observations

Star	Scanner 1			Scanner 2		
λ Lep	1969	Sept.	29.3070	1971	Aug.	5.8016
	1969	Sept.	29.3154	1971	Aug.	5.9406
η UMa	1969	July	19.1591	1971	July	4.3448
	1969	July	19.1698	1971	July	4.4145
	1969	July	19.2287			
	1969	July	19.9350			
ζ Dra	1969	July	16.8752	1971	April	20.8572
				1971	April	21.3443
				1971	April	21.4132
				1971	April	21.4836
				1971	April	21.5531
				1971	April	21.6222
α Leo	1969	May	18.3083	1971	May	15.4984
	1969	May	18.3779			
γ UMa				1971	May	16.2639
				1971	May	16.3336
α Lyr	1970	March	23.5036	1971	Sept.	18.0903
	1970	March	23.5633			
	1970	March	23.5733			

TABLE 3

Estimated Radii of the Stars

Star	Spectral Type	Distance (pc)	Source for Distance	$R/R_\odot$ (eqt. 4)	$R/R_\odot$ HB *et al.*
λ Lep	B0.5 V	455	$M_V = -4.0$	9.42	
η UMa	B3 V	51.7	$M_V = -1.7$	4.54	
ζ Dra	B6 III	69.2	$M_V = -1.0$	4.24	
α Leo	B7 V	22.5	$M_V = -0.40$	3.44	3.8 ± 1.0
γ UMa	A0 V	19.4	$M_V = +1.0$	2.74	
α Lyr	A0 V	8.13	$\pi = 0''.123$	2.69	3.03 ± 0.22
α CMa	A1 V	2.67	$\pi = 0''.375$	1.78	1.76 ± 0.04

TABLE 4

Absolute Fluxes for η UMa Compared with Predicted Fluxes

λ(Å)	Opal *et al.* (1968)	This Paper	Model (18000°)	λ(Å)	Opal *et al.* (1968)	This Paper	Model (18000°)
1300	93	54	180	1600	71	70	116
1400	84	64	157	1700	79	64	101
1500	72	65	134	1800	88	62	89

The unit of flux is 10^{-10} erg cm^{-2} s^{-1} Å^{-1}

CAPTIONS FOR THE FIGURES

Fig. 1 - The ultraviolet flux envelope of λ Lep. The data from OAO-II Scanner 2 are shown as dots connected by a line; those from Scanner 1 as open circles. The reference flux envelope is from the Van Citters and Morton (1970) model with He/H = 0.15, $\theta_e = 0.200$, log g = 4.0. The unit of flux is 10^{-10} erg $cm^{-2}s^{-1}Å^{-1}$.

Fig. 2 - The near ultraviolet and visible flux of λ Lep. Results from OAO-II Scanner 1 are shown by open circles; the ground-based observations of Hardorp and Scholz (1970) by crosses. The unit of flux is 10^{-10} erg $cm^{-2}s^{-1}Å^{-1}$. The scales for the upper curve are on the top and on the right; those for the lower curve on the bottom and to the left.

Fig. 3.- Stellar flux envelopes relative to representative predicted flux envelopes.

Fig. 4 - The flux envelope of η UMa. The data from OAO-II Scanner 2 are shown by dots connected by a line; that from Scanner 1 by unconnected dots. The ground-based observations of Schild, Peterson and Oke (1971) are shown by open circles. The reference flux envelope is from the Klinglesmith (1971) model with parameters (18000°, 4.0, 2/3, 1/3). The unit of flux is 10^{-10} erg $cm^{-2}s^{-1}Å^{-1}$.

Fig. 5 - The flux envelope of γ UMa. The data from OAO-II Scanner 2 are shown by dots connected by a line; those from the observations of Schild, Peterson and Oke (1971) by unconnected dots. The reference flux envelope is from an unpublished Klinglesmith model with Teff = 9750^o, log g = 4.0, X = 0.70034, Y = 0.27812 and X_{Si} = 0.02154. The unit of flux is 10^{-10} erg $cm^{-2}s^{-1}Å^{-1}$.

Fig. 6 - The flux envelope of α Lyr. The data from OAO-II Scanner 2 are shown by dots connected by a line; those from Scanner 1 by filled triangles. The ground-based observations of Oke and Schild (1970) are shown by unconnected dots while the modified observations of Hayes (1970) are shown by crosses. The reference flux envelope given by a continuous line is the same as in Fig. 5 but scaled to fit α Lyr. That given by a broken line is from Schild, Peterson and Oke (1971). The unit of flux is 10^{-10} erg $cm^{-2}s^{-1}Å^{-1}$.

Fig. 7. - Stellar flux envelopes for γ UMa, α Lyr and α CMa relative to the predicted flux envelope from the Klinglesmith model with T_{eff} = 9750^o, log g = 4.0, X = 0.70034, Y = 0.27812 and X_{Si} = 0.02154.

Fig 8. - The flux envelope of α CMa. The data read from Stecher's (1970) curves are shown by open circles, those of Evans (1971) by crosses. The ground-based results of Schild, Peterson and Oke are given by filled circles. The reference flux envelope is the same as in Fig. 5 but scaled to fit α CMa. The unit of flux is 10^{-9} erg $cm^{-2} s^{-1} Å^{-1}$.

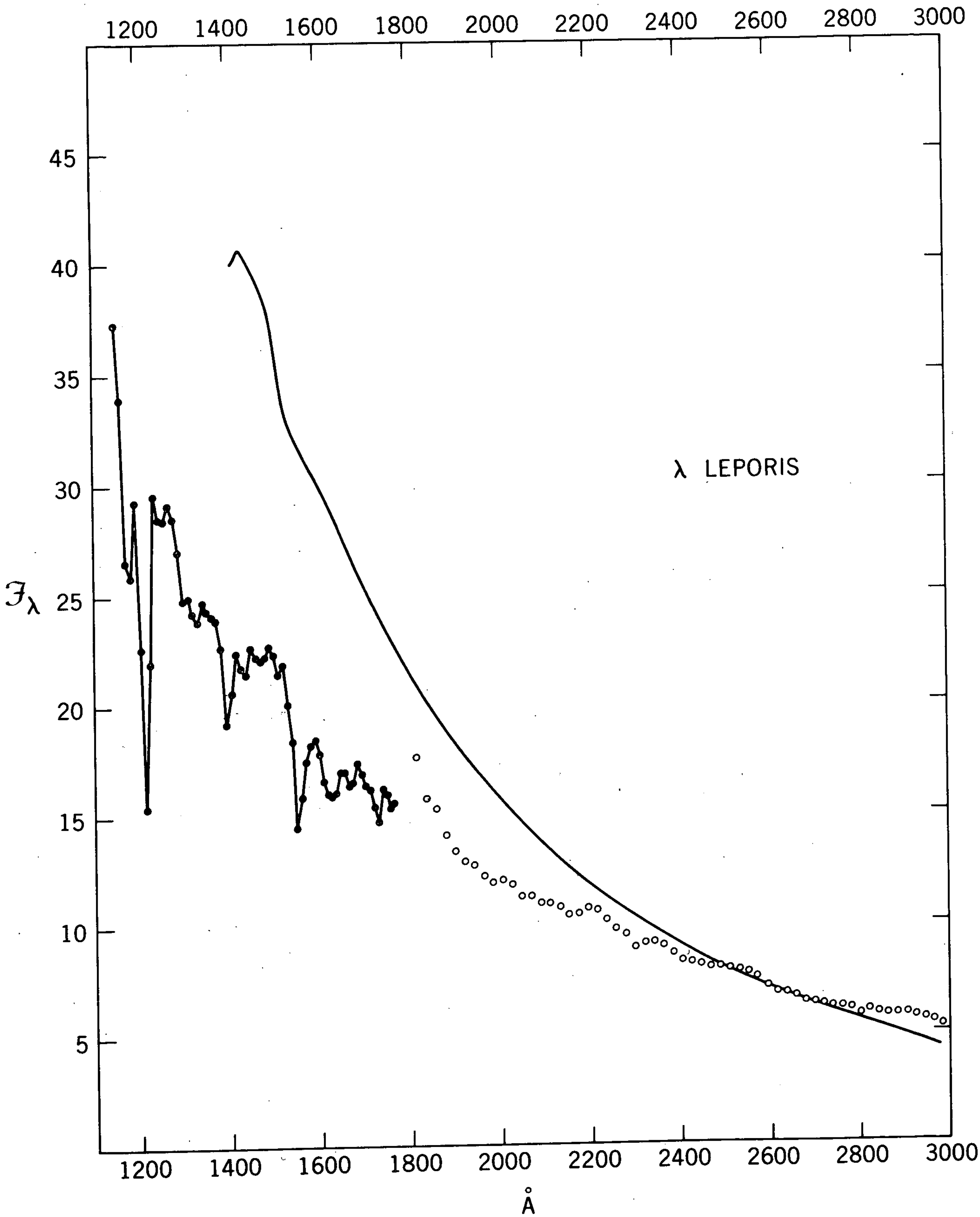

1200
1400
1600
1800
2000
2200
2400
2600
2800
3000
45
40
35
30
25
20
15
10
5
$\mathcal{F}_\lambda$
λ LEPORIS
Å

FIGURE 1

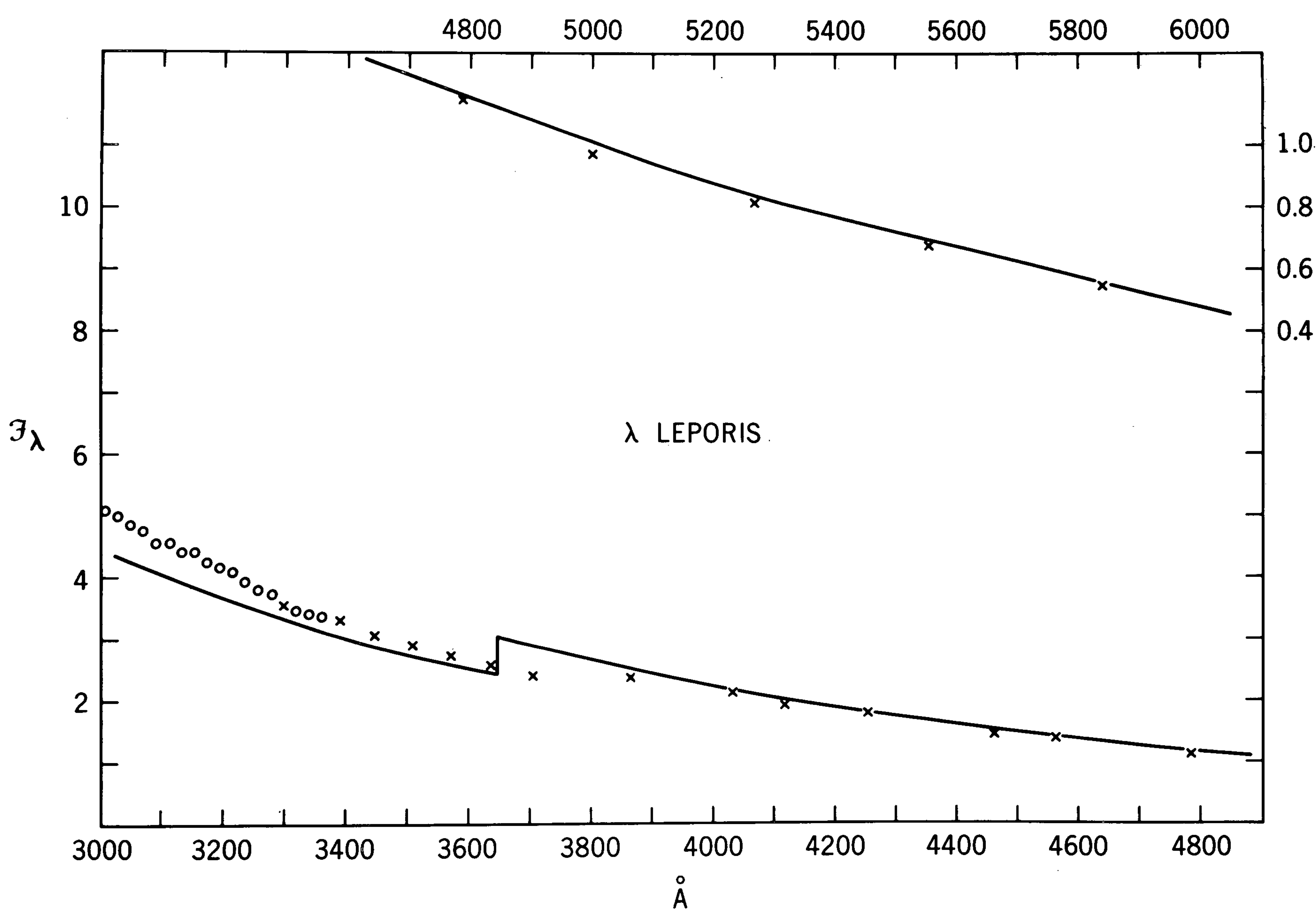

4800
5000
5200
5400
5600
5800
6000
1.0
0.8
0.6
0.4
10
8
6
4
2
$\mathcal{F}_\lambda$
λ LEPORIS
3000
3200
3400
3600
3800
4000
4200
4400
4600
4800
Å

FIGURE 2

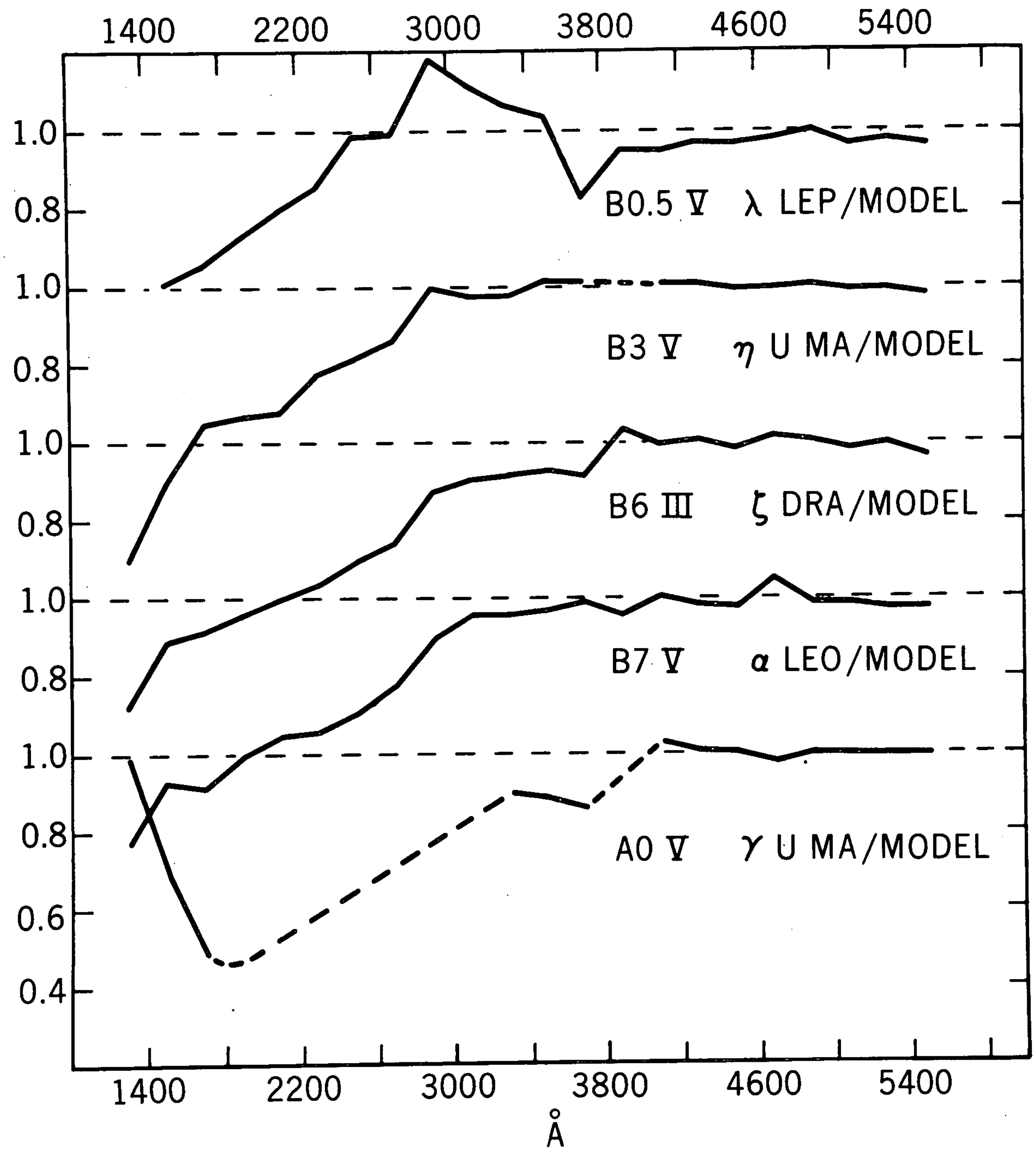
1400
2200
3000
3800
4600
5400
1.0
0.8
1.0
0.8
1.0
0.8
1.0
0.8
1.0
0.8
0.6
0.4
B0.5 V λ LEP/MODEL
B3 V η U MA/MODEL
B6 III ζ DRA/MODEL
B7 V α LEO/MODEL
A0 V γ U MA/MODEL
1400
2200
3000
3800
4600
5400
Å

FIGURE 3

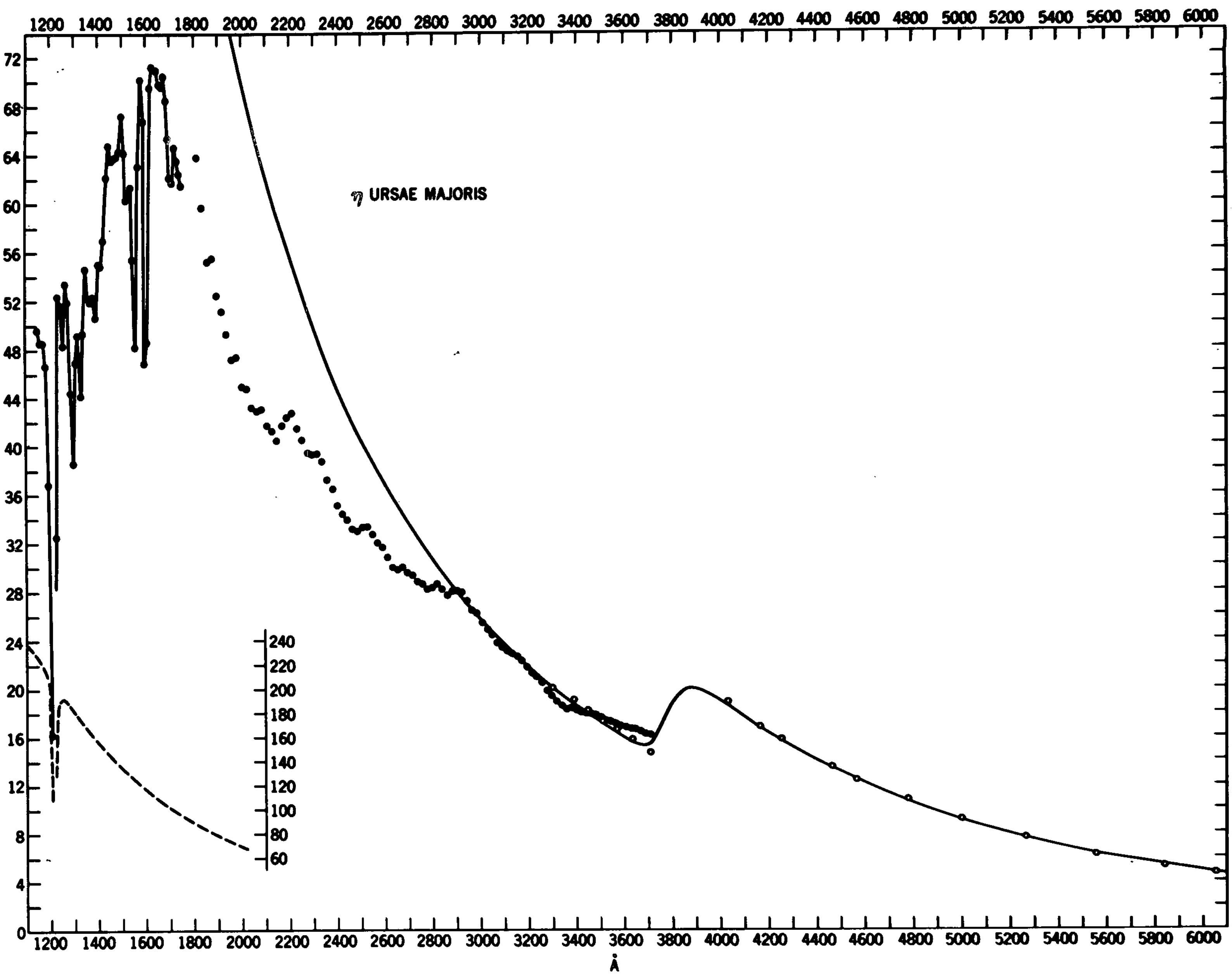

FIGURE 4

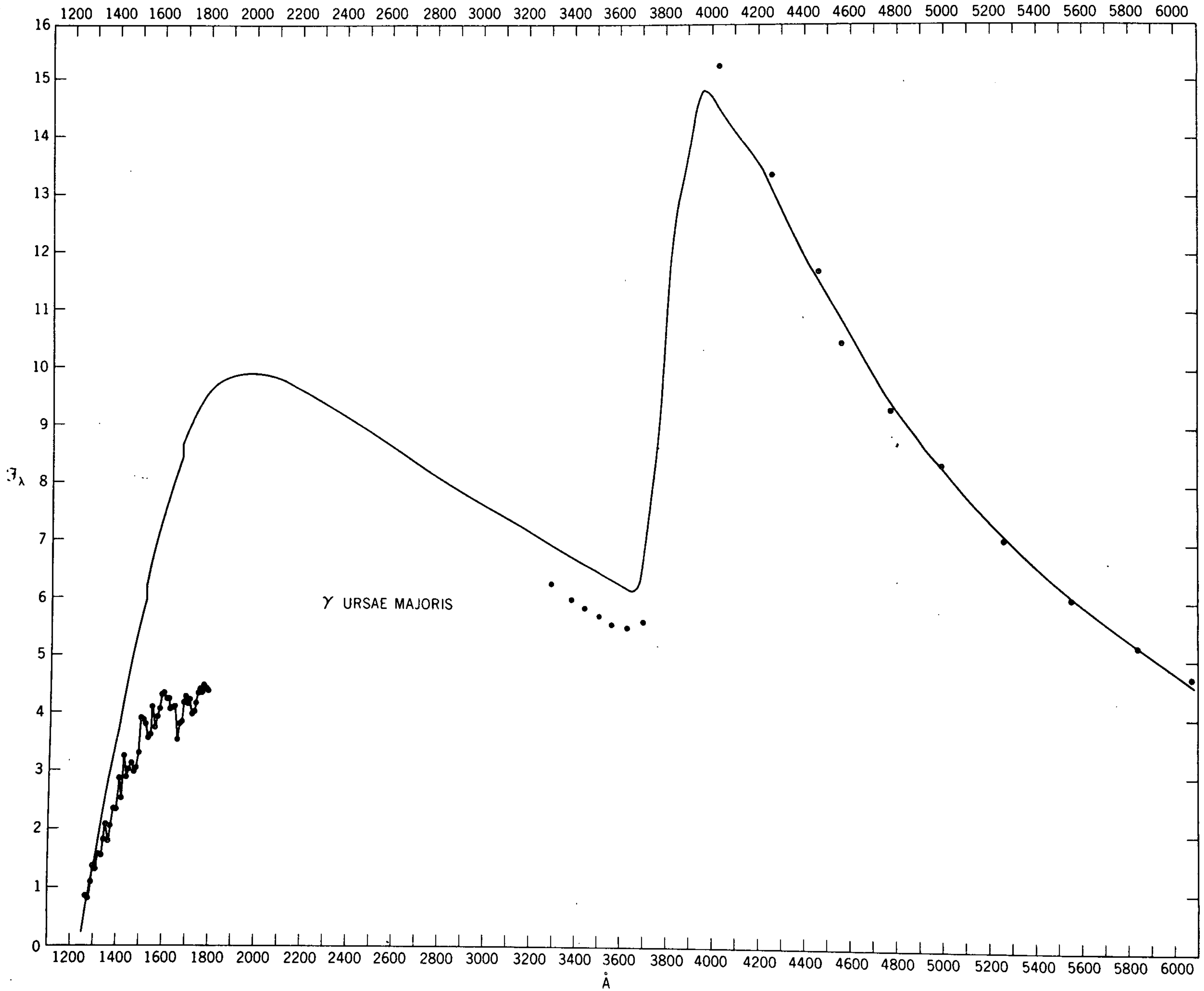

FIGURE 5

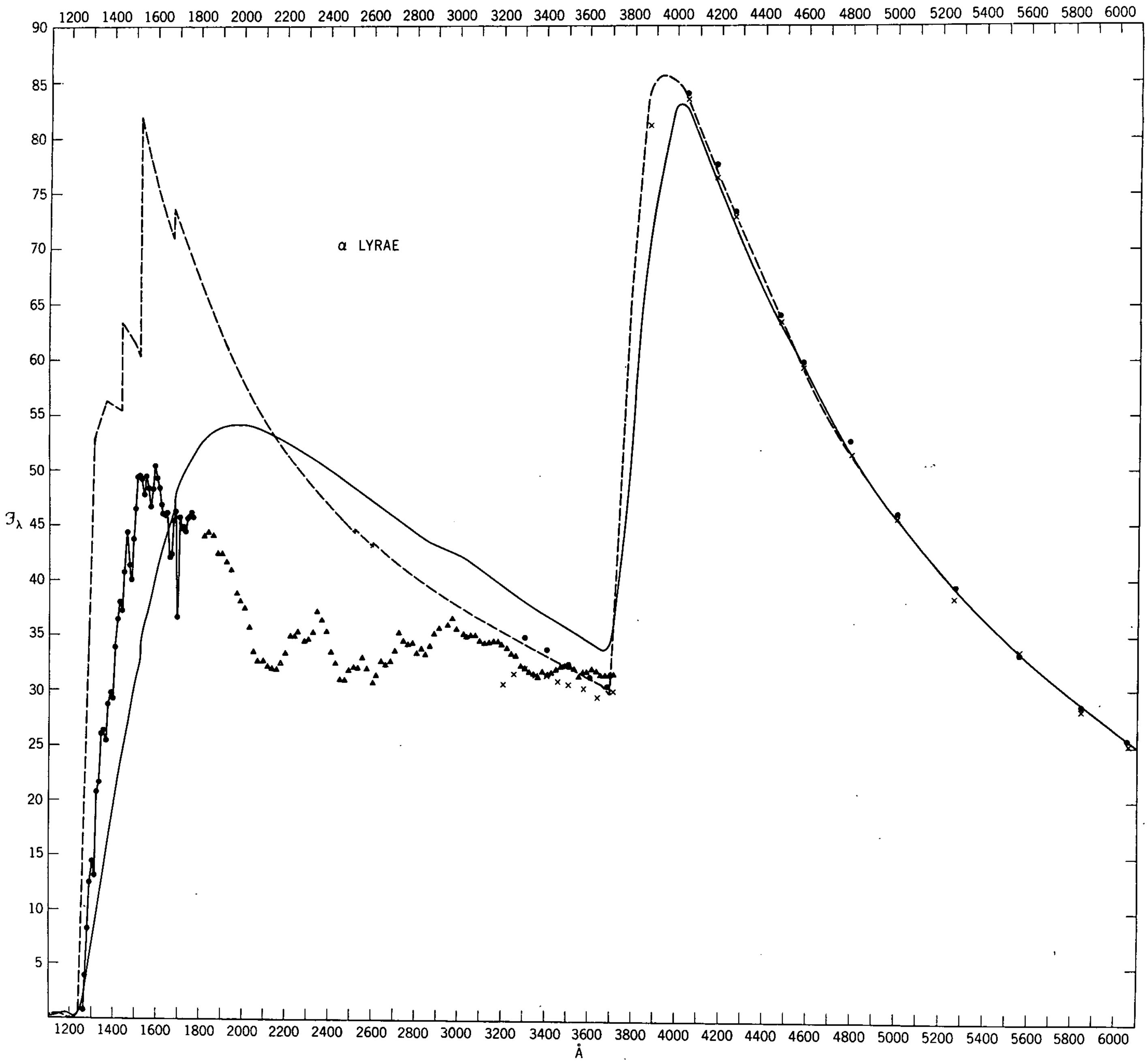

FIGURE 6

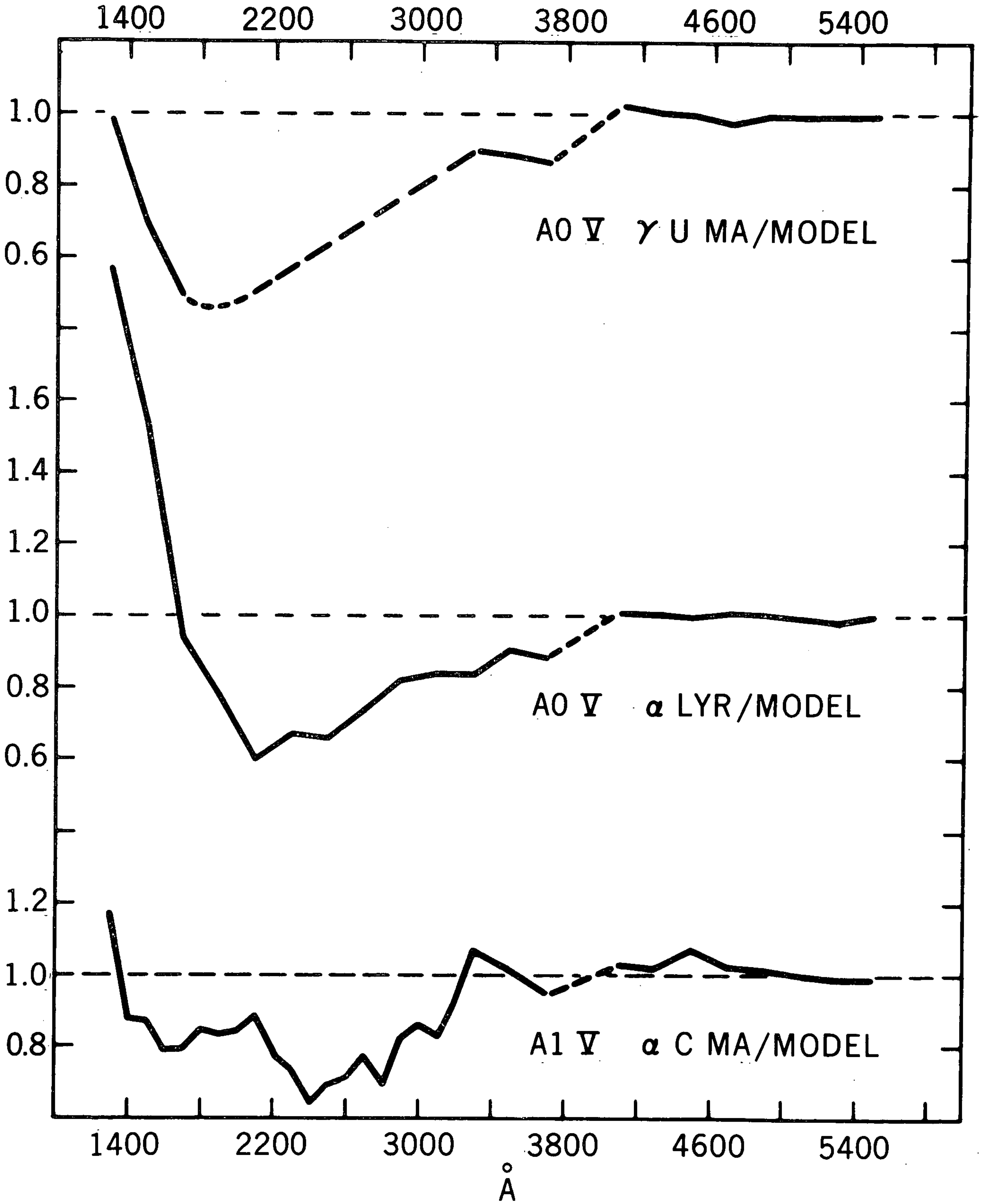

1400
2200
3000
3800
4600
5400
1.0
0.8
0.6
A0 V γ U MA/MODEL
1.6
1.4
1.2
1.0
0.8
0.6
A0 V α LYR/MODEL
1.2
1.0
0.8
A1 V α C MA/MODEL
1400
2200
3000
3800
4600
5400
Å

FIGURE 7

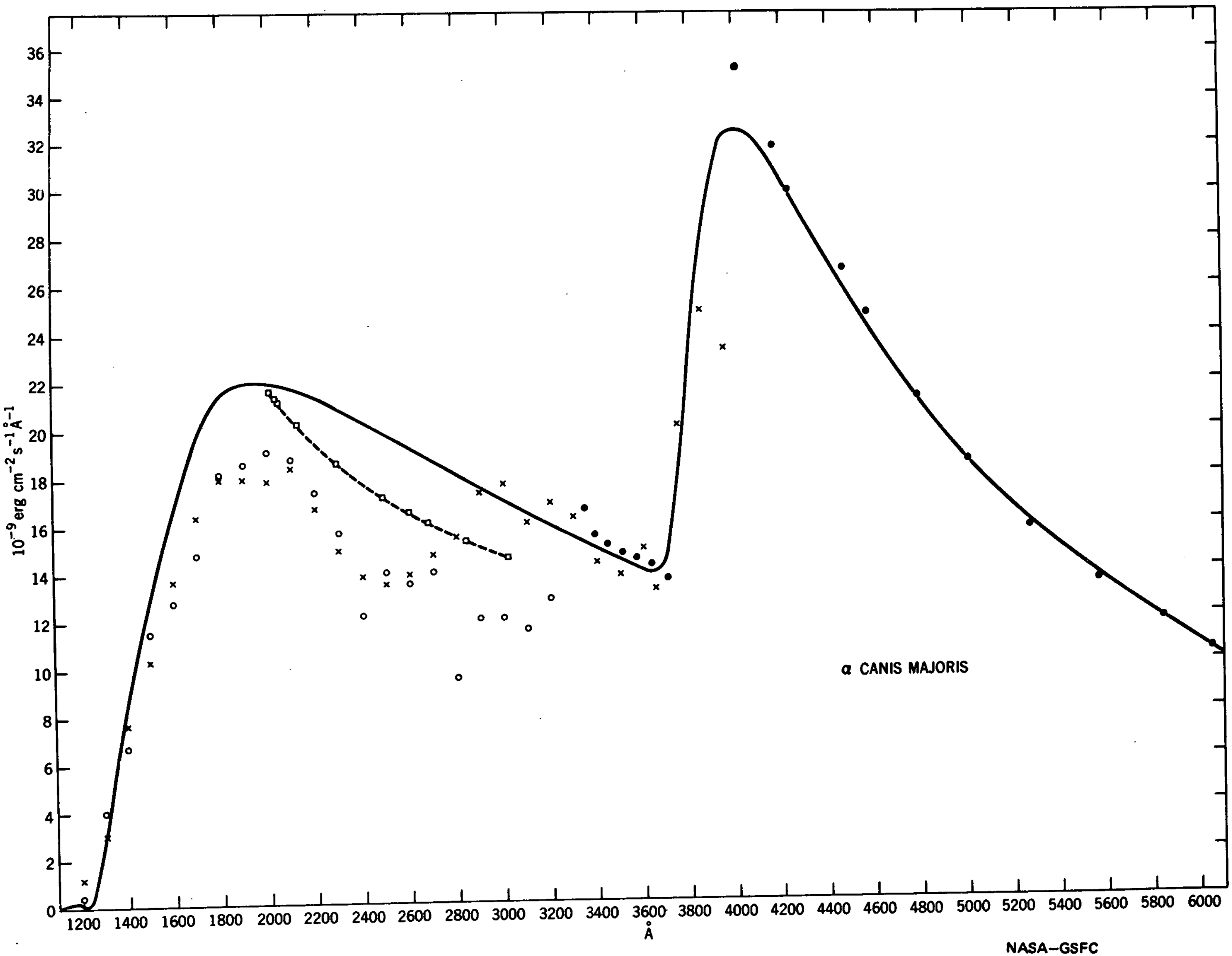

FIGURE 8